A Journal of the Gesellschaft Deutscher Chemiker

Angewandte International Edition Chemie

GDCh

www.angewandte.org

Accepted Article

Title: Mass Spectrometric Study of Acoustically Levitated Droplet Illuminates Molecular-Level Mechanism of Photodynamic Therapy for Cancer involving Lipid Oxidation

Authors: Chaonan Mu, Jie Wang, Kevin M. Barraza, Xinxing Zhang, and J.L. Beauchamp

To be cited as: *Angew. Chem. Int. Ed.* 10.1002/anie.201902815
Angew. Chem. 10.1002/ange.201902815

Link to VoR: http://dx.doi.org/10.1002/anie.201902815
http://dx.doi.org/10.1002/ange.201902815

WILEY-VCH

10.1002/anie.201902815

WILEY-VCH

COMMUNICATION

Mass Spectrometric Study of Acoustically Levitated Droplet Illuminates Molecular-Level Mechanism of Photodynamic Therapy for Cancer involving Lipid Oxidation

Chaonan Mu, Jie Wang, Kevin M. Barraza, Xinxing Zhang* and J. L. Beauchamp*

Abstract: Even though the general mechanism of photodynamic therapy for cancer is known, the details and consequences of the reactions between the photosensitizer generated singlet oxygen and substrate molecules remain elusive at the molecular level. Using temoporfin as the photosensitizer, here we combine field-induced droplet ionization mass spectrometry and acoustic levitation techniques to study the "wall-less" oxidation reactions of 18:1 cardiolipin and POPG mediated by singlet oxygen at the air-water interface of levitated water droplets. For both cardiolipin and POPG, every unsaturated oleyl chain is oxidized into an allyl hydroperoxide, which surprisingly is immune to further oxidation. This is attributed to the increased hydrophilicity of the oxidized chain, attracting it toward the water phase, increasing membrane permeability and eventually triggering cell death.

More than a century has passed since Meyer-Betz performed the very first study of photodynamic therapy (PDT) using porphyrins on his own hands.[1,2] Subsequent research has led to the development of PDT drugs which have been approved for clinical use.[2,3] The mechanism of PDT is generally believed to proceed as follows.[4] Upon absorption of light, a photosensitizer (PS) is excited from the ground singlet state to an excited singlet state, then transformed into a relatively long-lived triplet state by intersystem crossing. This triplet could oxidize the substrate by one electron or abstract H atom from the substrate, followed by various O_2 mediated oxidation pathways such as the formation of O_2^-, HO_2^-, H_2O_2 and OH (type I), or transfer its energy to an adjacent oxygen molecule, forming singlet oxygen (SO), $^1O_2$ ($^1\Delta_g$). SO will react with molecules that are in close proximity to the area of its generation (type II). Type I and Type II reactions occur simultaneously, with variable branching ratio depending on types and concentrations of the PS, substrate, and oxygen. PDT attacks cancer cells in different manners including direct tumor cell killing by triggering apoptosis, vascular damage and the activation of immune response.[2–6]

Although the general mechanisms of PDT targeting unsaturated phospholipids,[7–11] residues of proteins or peptides,[12] and nucleic acid components of DNA and RNA[13] are known, the details of reactions between PS generated SO and substrate molecules at the molecular level remain elusive[14] especially at the early stage of the reaction. This is because the nascent products stemming from SO oxidation are themselves highly reactive, easily degrading or evolving into other products with time or during sample characterization.[15] Frequently used characterization methods for lipid oxidation, such as oxygen consumption, fluorescence, and chromatographic measurements are either indirect or involve extensive sample handling and transfer.[16,17] In view of this, here we report a new methodology that combines two techniques, field–induced droplet ionization mass spectrometry (FIDI-MS) and acoustic levitation (AL) to study the photosensitized oxidation of 18:1 cardiolipin (CL) and 1-palmitoyl-2-oleoyl-sn-glycero-3-phospho-(1'-rac-glycerol) (POPG) at the air-water interface of levitated droplets. These two substrates are selected to represent a major target of PDT, unsaturated phospholipids. 5, 10, 15, 20-tetra(m-hydroxyphenyl)chlorin), also known as temoporfin, is selected to be the PS in this study for its lipophilic nature, high quantum yield and benign, tissue penetrating activation wavelength (652 nm).[18] Temoporfin has been approved in Europe for treatment of certain skin cancers and sold under the trade name Foscan®.[1] The FIDI-MS methodology[19–23] developed in our group has been proven to be interfacially sensitive, and it selectively samples molecules that are at the air-water interface after a well-defined reaction time. Previous FIDI-MS studies of interfacial chemistry have used hanging droplets.[21-23] Acoustically levitated droplets promise to be "wall-less" airborne reactors with no interference resulting from contact with a support,[24a] and sound is less invasive compared to other levitation techniques such as optic tweezer.[25] AL coupled with other techniques, including mass spectrometry, laser ionization/desorption, electrochemistry, electrophoresis, chemiluminescence, UV/Vis and Raman spectroscopy, and chromatography has been applied to examine a wide range of scientific problems.[24] In this communication, for the first time, we combine FIDI-MS and AL to elucidate mechanistic aspects of PDT chemistry at the air-water interface.

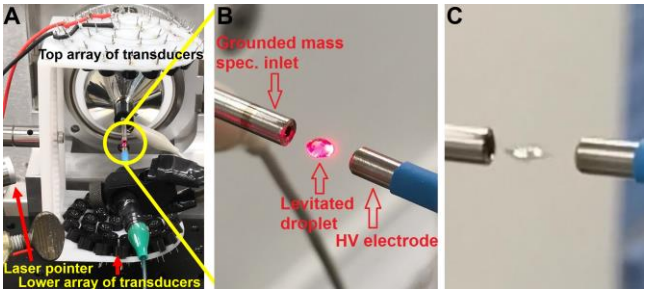

Figure 1. The experimental setup of AL coupled with FIDI-MS. (A) The overall arrangement of the levitator, FIDI electrodes, and mass spectrometer. (B) A levitated and illuminated droplet

[*] Chaonan Mu, Jie Wang, Dr. Prof. X. Zhang,
Key Laboratory of Advanced Energy Materials Chemistry (Ministry of Education), Renewable Energy Conversion and Storage Center (ReCAST),
College of Chemistry, Nankai University
Tianjin 300071 (China)
E-mail: zhangxx@nankai.edu.cn
Kevin M. Barraza, Dr. Prof. J. L. Beauchamp,
Noyes Laboratory of Chemical Physics and the Beckman Institute
California Institute of Technology
Pasadena, California, 91125 (USA)
E-mail: jlbchamp@caltech.edu

Supporting information for this article is given via a link at the end of the document.

10.1002/anie.201902815

sandwiched by the two FIDI electrodes, one of which is the atmospheric pressure sampling input of the mass spectrometer, and the other is the high voltage electrode. (C) Bipolar Taylor cones form upon triggering the FIDI voltage. A closer picture of the levitator and the acoustic field it emits are provided in Figure S1.

Details of the experimental methods are provided in the supporting information. The acoustic levitator in the current study is based on a design by Marzo *et al*.[26] It features single-axis levitation using two arrays (36 transducers mounted on a partial hemisphere in each array) of 40 kHz ultrasonic transducers sandwiching the levitated object. We built a slightly modified version to mount it in close proximity of the extended inlet of a Thermo-Fisher LTQ-XL mass spectrometer (Figures 1A, S1). A water droplet (~2 mm o.d., ~4 µL) containing a mixture comprising 100 µM CL or POPG and 50 µM temoporfin is trapped in the center node (Figure 1B) of the nodes generated by the standing wave resulting from interference of the sound waves originating from the top and lower arrays of transducers. This levitated droplet is illuminated by a laser pointer (650 nm, 0.345 mW/cm^2, Figure S2), and placed between two hollow rod electrodes separated by ~10 mm, with the ground electrode being the mass spectrometer inlet and the high voltage electrode being connected to a high voltage pulser (4-7 kV, 5 ms, variable polarity). The red light remains on for a variable time period, usually several minutes, for the photodynamic reactions to take place. Upon triggering the high voltage, set slightly above the threshold for field induced droplet ionization, the electric field induces a dipole in the droplet that interacts with the applied field to stretch the levitated droplet until bipolar Taylor cones form at opposite ends, ejecting charged submicron progeny droplets of opposite polarity toward the appropriately biased electrodes (Figure 1C). The progeny droplets ejected into the mass spectrometer yield ions that are subjected to mass analysis and structural characterization using collision-induced dissociation (CID). Figure 1C is a frame taken with a Huawei® Mate 10 Pro smart phone at 240 frames per second.

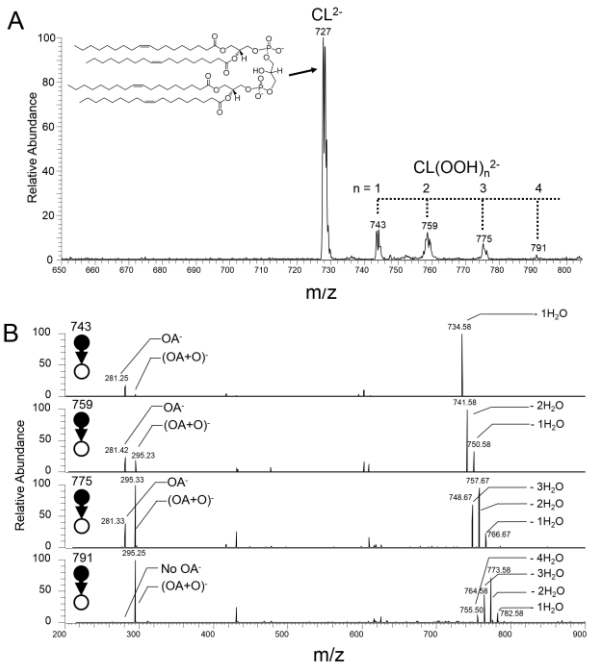

Figure 2. (A) FIDI-MS spectrum of CL oxidized by SO after exposure to red light for 4 mins. The products $CL(OOH)_{1\text{-}4}^{2-}$ are observed. (B) CID products of $CL(OOH)_{1\text{-}4}^{2-}$ showing that hydroperoxide group are distributed on different oleyl chains of CL.

Known to comprise a major component of the inner cell wall of mitochondria, cardiolipin is selected as a representative phospholipid in this study. Peroxidation of CL releases cytochrome C from the membrane, which in turn triggers apoptosis.[27] Figure 2A presents the structure of 18:1 CL and the FIDI-MS spectrum of the oxidation products after 4 mins exposure to the red light. A CL molecule possesses two negative charges and four unsaturated oleyl chains. According to the well-known mechanism of SO reaction with olefins,[28] all of these four unsaturated chains should be converted to allyl hydroperoxide functionality, and accordingly we observe four products: $CL(OOH)_{1\text{-}4}^{2-}$ (mechanism presented in Figure 5A). Approximately 26.5% of all the molecules are oxidized by adding at least one -OOH group. Control experiments with light off result in no oxidation. Other studies[7-9,11,15] have shown that photosensitized oxidation of unsaturated lipids can result in many other products such as alcohols, ketones and aldehydes, which might involve further degradation of the allyl hydroperoxide product. But here only the nascent allyl hydroperoxide products are observed, and no C=C double bond cleavage products are present at the lower m/z side of the spectrum, manifesting the efficacy of the combined levitated droplet and FIDI-MS analysis as being able to detect and characterize nascent reaction products at an early stage of photocatalytic oxidation.

An obvious question is whether or not the C=C double bond of the allyl hydroperoxide product is further oxidized by reaction with an additional SO. Alternatively stated, are the -OOH groups in the products distributed on different oleyl chains of CL, or do some of them occupy the same oleyl chain? To answer this question, we performed the CID analyses of the $CL(OOH)_{1\text{-}4}^{2-}$ products (Figure 2B). At the higher m/z region of the spectra, up to n water molecules are lost in each $CL(OOH)_n^{2-}$ parent ion, indicating that there are indeed n -OOH groups in each $CL(OOH)_n^{2-}$.[29] The lower m/z portion is the key to answer the question raised above. For $CL(OOH)_{1\text{-}3}^{2-}$, the collisionally dissociated oleic acid fragment (OA^-), resulting from the unoxidized oleyl chain of CL, is observed concomitantly with the loss of H_2O product of $OA(OOH)^-$, i.e. $(OA+O)^-$, from the oxidized oleyl chain of CL. The intensities of $(OA+O)^-$ relative to those of OA^- increases with n. Especially in $CL(OOH)_2^{2-}$, the intensities of $(OA+O)^-$ and OA^- are almost identical, indicating that two oleyl chains of CL are oxidized by adding -OOH, while the other two stay intact. In the CID spectrum of $CL(OOH)_4^{2-}$, no OA^- was observed, suggesting that the four -OOH moieties are equally distributed on all four unsaturated chains of CL. To conclude, every unsaturated oleyl chain in a CL molecule is singly oxidized by SO to form an allyl hydroperoxide, and the allyl group is immune to further oxidation. Additional evidence for this assertion is that no $CL(OOH)_n^{2-}$ (n>4) was observed in the spectrum. We propose that the failure to observe further oxidation of the allyl hydroperoxide product has implications for events that occur at the lipid-water interface subsequent to oxidation. This is further discussed below and illustrated in Figure 5B. Proposed mechanisms for loss of H_2O from the CID of an allyl hydroperoxide are provided in Figure S3.

Figure 3A presents the structure of the POPG parent anion and FIDI-MS spectrum of the oxidation products after 4 mins exposure to red light, using conditions analogous to those employed for CL oxidation. A POPG molecule possesses one negative charge, one unsaturated oleyl chain and one saturated palmitoyl chain. Only the product $POPG(OOH)^-$ was observed after oxidation, comprising 26.4% of the observed ions. Again, the oleyl chain was not oxidized twice. CID of $POPG(OOH)^-$ in Figure 3B shows the loss one H_2O, the fragments of palmitic acid (PA^-), $(OA+O)^-$, and a small amount of $OA(OOH)^-$. The existence of PA^- suggests that the saturated hydrocarbon chain does not react with SO. To further confirm the identity of the -OOH group, H/D exchange experiments were performed by using a droplet comprising D_2O. Since $POPG^-$ is singly charged, the H/D exchange can be better observed than in CL due to spectral resolution considerations. $POPG^-$ has two exchangeable H atoms of the two hydroxyl groups on the terminal glycerol moiety. $POPG(OOH)^-$ has one more exchangeable H atom on -OOH. Figure 4 presents the H/D exchange results of both $POPG^-$ and $POPG(OOH)^-$. Up to 2 Da shift and 3 Da shift can be observed for $POPG^-$ and $POPG(OOH)^-$, respectively, indicating that -OOH is indeed present in the molecule. After substracting the ion intensities of the isotopic contributions from the lower m/z peaks, in the lower panel of Figure 4, quantitatively, 19% of the $POPG^-$ molecules remain intact, 50% have one H atom exchanged by D, and 31% have both H atoms exchanged by D. For $POPG(OOH)^-$, 8% have no H/D exchange, 32% have one H atom exchanged by an D atom, 43% have two H atoms exchanged by D, and 17% have all three H atoms exchanged by D. The FIDI mass spectrum in cation mode showing the oxdation by SO of temoporfin (photobleaching) after 4 mins of light exposure is provided in Figure S4. Only 10% of temoporfin is oxidized by adding 32 Da, indicating that it is less reactive toward self oxidation compared to the double bonds in the lipids, making it a robust PS.

Figure 5 presents reaction mechanisms from which some insights into how PDT works can be derived. Figure 5A is the well-accepted mechanism of SO reacting with a C=C double bond, which is directly applicable to CL and POPG. Basically a double bond adds one SO molecule, and the terminal O atom then abstracts one H atom from either of the neighboring carbon atoms, resulting in an allyl hydroperoxide molecule where the C=C bond is shifted by one carbon from the original position. Next we discuss the observation that subsequent attack by SO preferentially occurs at a different oleyl chain instead of the allyl hydroperoxide. The structures of CL and temoporfin are drawn according to their real relative sizes in Figure 5B. Temoporfin is lipophilic, so it prefers to reside in the oil phase, i.e. the lipid monolayer. [18] Consequently, the SO molecules generated by the PS are in very close proximity to the targeted site, namely the C=C double bond centered on the oleyl chains. Upon oxidation, the resultant hydroperoxide moiety, with increased hydrophilicity, drags the fatty acid chain out of the "war zone" into the water phase in order to form hydrogen bonds with water molecules (Figure 5B). The lifetime of SO *in vivo* was reported to be a very short time ranging from nanoseconds[30] to microseconds.[31] Therefore, SO is supposedly left to attack the C=C double bonds remaining in close proximity, resulting in the even distribution of -OOH on different oleyl chains. Another evidence for this "floating" hydroperoxide scenario is the H/D exchange on –OOH observed in Figure 4B: only when the –OOH is in the water phase can it have a better chance to interact with D_2O. The conformational change of the -OOH decorated fatty acid chain will lead to an increase in the average area per lipid and to a decrease of the layer thickness and packing density, which will eventually result in a leaky membrane and cell death. The floating hydroperoxide scenario has been studied by various *in-silico* molecular dynamics simulations,[32] but our experiment provides direct evidence for this subtle mechanism of PDT at the molecular level.

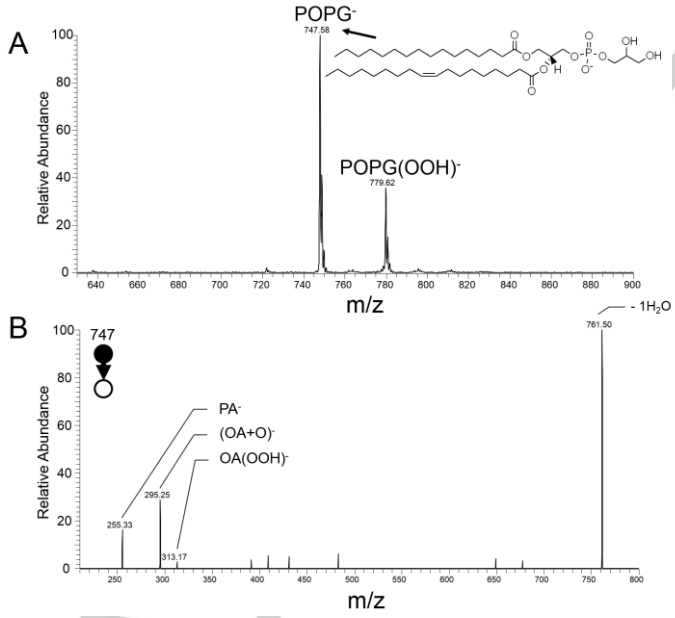

Figure 3. (A) FIDI-MS spectrum of POPG oxidized by SO after exposure to red light for 4 mins. The product $POPG(OOH)^-$ is observed. (B) CID products of $POPG(OOH)^-$ showing that the oleyl chain is oxidized but the palmitoyl chain remains intact.

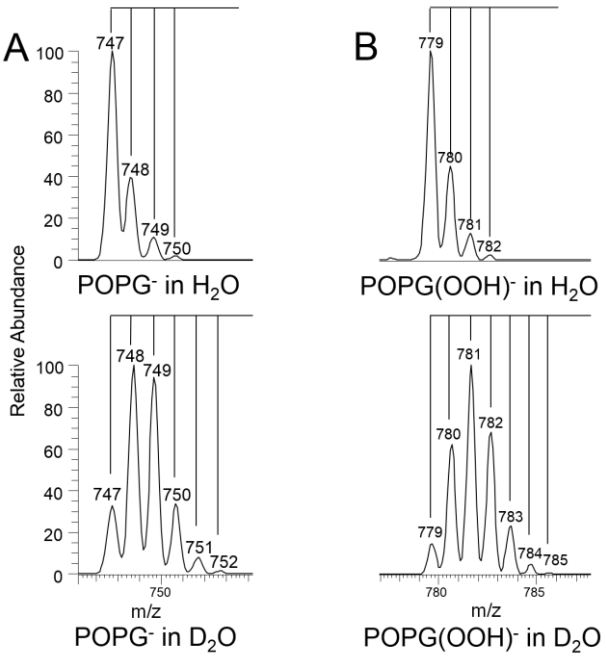

Figure 4. (A) FIDI-MS spectra of $POPG^-$ in H_2O and D_2O solutions. (B) FIDI-MS spectra of $POPG(OOH)^-$ in H_2O and D_2O solutions.

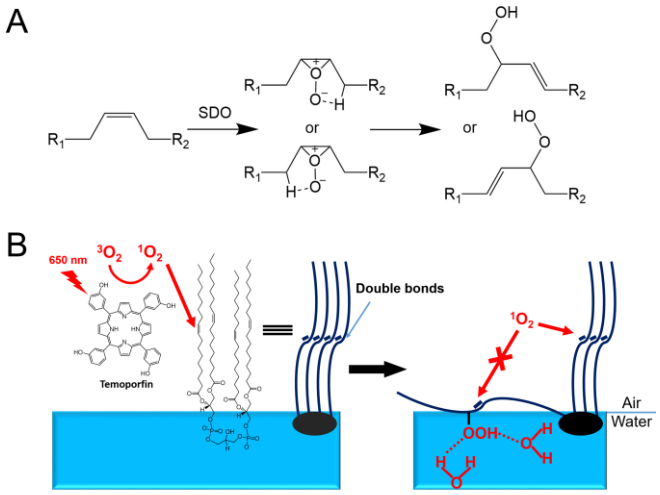

Figure 5. (A) Mechanism of the C=C double bonds of CL or POPG being oxidized by SO. (B) Cartoon showing the allyl hydroperoxide resulted from SO oxidation moving out of the hydrophobic lipid environment into the water phase in order to form hydrogen bonds with water molecules. POPG behaves similarly. The photosensitizer temoporfin is embedded in the hydrophobic portion of the lipid environment.

Keywords

Lipid oxidation; Photodynamic therapy; Mass spectrometry; Air-water interface; Acoustic levitation

Acknowledgements

This work was supported by the Beckman Institute at Caltech and by NSF grant CHE–1508825 (J.L.B.). This work is dedicated to the 100th anniversary of Nankai University.

Keywords: photodynamic therapy • singlet oxygen • photosensitizer • lipid oxidation • peroxidation

[1] F. Meyer–Betz, *Dtsch Arch. Klin.* **1913**, *112*, 476–503.
[2] D. E. J. G. J. Dolmans, D. Fukumura, R. K. Jain, *Nat. Rev. Cancer* **2003**, *3*, 380–387.
[3] R. R. Allison, C. H. Sibata, *Photodiagnosis Photodyn. Ther.* **2010**, *7*, 61-75.
[4] M. S. Baptista, J. Cadet, P. D. Mascio, A. A. Ghogare, A. Greer, M. R. Hamblin, C. Lorente, S. C. Nunez, M. S. Ribeiro, A. H. Thomas, M. Vignoni, T. M. Yoshimura, *Photochem. Photobiol.* **2017**, *93*, 912-919.
[5] C. M. Moore, D. Pendse, M. Emberton, *Nat. Clin. Pract. Urol.* **2009**, *6*, 18–30.
[6] (a) A. P. Castano, T. N. Demidova, M. R. Hamblin, *Photodiagnosis Photodyn. Ther.* **2004**, *1*, 279–293; (b) **2005**, *2*, 1–23; (c) **2005**, *2*, 91–106.
[7] A. Reis, C. M. Spickett, *Biochim. Biophys. Acta* **2012**, *1818*, 2374–2387.
[8] J. Kim, P. E. Minkler, R. G. Salomon, V. E. Anderson, C. L. Hoppel, *J. Lipid Res.* **2011**, *52*, 125–135.
[9] I. O. L. Bacellar, M. C. Oliveira, L. S. Dantas, E. B. Costa, H. C. Junqueira, W. K. Martins, A. M. Durantini, G. Cosa, P. D. Mascio, M. Wainwright, R. Miotto, R. M. Cordeiro, S. Miyamoto, M. S. Baptista, *J. Am. Chem. Soc.* **2018**, *140*, 9606–9615.
[10] A. Wolnicka–Glubisz, M. Lukasik, A. Pawlak, A. Wielgus, M. Niziolek–Kierecka, T. Sarna, *Photochem. Photobiol. Sci.* **2009**, *8*, 241−247.
[11] T. Melo, N. Santos, D. Lopes, E. Alves, E. Maciel, M. A. F. Faustino, J. P. C. Tome, M. G. P. M. S. Neves, A. Almeida, P. Domingues, M. A. Segundo, M. R. M. Domingues, *J. Mass Spectrom.* **2013**, *48* (12), 1357−1365.
[12] A. Michaeli A, J. Feitelson, *Photochem Photobiol.* **1994**, *59*, 284–289.
[13] S. Rangasamy, H. Ju, S. Um, D. -C. Oh, J. M. Song, *J. Med. Chem.*, **2015**, *58*, 6864–6874.
[14] I. O. L. Bacellar, T. Tsubone, C. Pavani, M. Baptista, *Int. J. Mol. Sci.* **2015**, *16*, 20523−20559.
[15] M. M. Gaschler, B. R. Stockwell, *Biochem. Biophys. Res. Co.* **2017**, *482*, 419–425.
[16] L. E. Greene, R. Lincoln, G. Cosa, *Free Radic. Biol. Med.* https://doi.org/10.1016/j.freeradbiomed.2018.04.006
[17] J. M. C.Gutteridge, B. Halliwell *Trends Biochem. Sci.* **1990,** *15*, 129–135.
[18] (a) M. O. Senge, J. C. Brandt, *Photochem. Photobio.* **2011**, *87*, 1240–1296; (b) J. Y. Chen, N. K. Mak, C. M N. Yow, M. C. Fung, L. C. Chiu, W. N. Leung, N. H. Cheung, *Photochem. Photobio.* **2000**, *72*, 541-547; (c) P. Cramers, M. Ruevekamp, H. Oppelaar, O. Dalesio, P. Baas, F. A. Stewart, *Br. J. Cancer* **2003**, *88*, 283–290.
[19] R. L. Grimm, J. L. Beauchamp, *J. Phys. Chem. B* **2003**, *107*, 14161–14163.
[20] R. L. Grimm, J. L. Beauchamp, *J. Phys. Chem. B* **2005**, *109*, 8244–8250.
[21] X. Zhang, K. M. Barraza, J. L. Beauchamp, *Proc. Natl. Acad. Sci.* **2018**, *115*, 3255–3260.
[22] X. Zhang, K. M. Barraza, K. T. Upton, J. L. Beauchamp, *Chem. Phys. Lett.* **2017**, *683*, 76–82.
[23] X. Zhang, K. M. Barraza, K. T. Upton, J. L. Beauchamp, *J. Am. Chem. Soc.* **2018**, *140*, 17492-17498.
[24] (a) A. Scheeline, R. L. Behrens, *Biophys. Chem.* **2012**, *165–166*, 1–12; (b) E. A. Crawford, C. Esen, D. A. Volmer, *Anal. Chem.* **2016**, *88*, 8396−8403; (c) C. Warschat, J. Riedel, *Rev. Sci. Instrum.* **2017**, *88*, 105108; (d) M. S. Westphall, K. Jorabchi, L. M. Smith, *Anal. Chem.* **2008**, *80*, 5847–5853; (e) A. Stindt, M. Albrecht, U. Panne, J. Riedel, *Anal. Bioanal. Chem.* **2013**, *405*, 7005–7010; (f) M. J. Petersson, J. Nilsson, L. Wallman, T. Laurell, J. Johansson, S. Nilsson, *J. Chromatog. B: Biomed. Sci. Applic.* **1998**, *714*, 39–46; (g) A. Scheeline, Z. Pierre, C. R. Field, M. D. Ginsberg, *Proc. of SPIE* **2009**, *7306*, 73061U; (h) E. T. Chainani, K. T. Ngo, A. Scheeline, *Anal. Chem.* **2013**, *85*, 2500−2506; (i) C. Warschat, A. Stindt, U. Panne, J. Riedel, *Anal. Chem.* **2015**, *87*, 8323−8327; (j) L. Puskar, R. Tuckermann, T. Frosch, J. Popp, V. Ly, D. McNaughton, B. R. Wood, *Lab Chip* **2007**, *7*, 1125–1131; (k) S. Santesson, J. Johansson, L. S. Taylor, I. Levander, S. Fox, M. Sepaniak, S. Nilsson, *Anal. Chem.* **2003**, *75*, 2177–2180; (l) R. J. Weber, C. J. Benmore, S. K. Tumber, A. N. Tailor, C. A. Rey, L. S. Taylor, S. R. Byrn, *Eur. Biophys. J.* **2012**, *41*,397–403; (m) S. Santesson, S. Nilsson, *Anal. Bioanal. Chem.* **2004**, *378*, 1704–1709; (n) J. Schenk, L. Trobs, F. Emmerling, J. Kneipp, U. Panne, M. Albrecht, *Anal. Methods* **2012**, *4*, 1252–1258.
[25] (a) A. Ashkin, J. M. Dziedzic, J. E. Bjorkholm, S. Chu, *Opt. Lett.* **1986**, *11*, 288–290; (b) A. Marzo, B. W. Drinkwater, *Proc. Natl. Acad. Sci.* **2019**, *116*, 84-89.
[26] A. Marzo, A. Barnes, B. W. Drinkwater, *Rev. Sci. Instrum.* **2017**, *88*, 085105.
[27] V. E. Kagan, V. A. Tyurin, J. Jiang, Y. Y. Tyurina, V. B. Ritov, A. A. Amoscato, A. N. Osipov, N. A. Belikova, A. A. Kapralov, V. Kini, I. I. Vlasova, Q. Zhao, M. Zou, P. Di, D. A. Svistunenko, I. V. Kurnikov, G. G. Borisenko, *Nat. Chem. Biol.* **2005**,*1*, 223–232.
[28] H. H. Wasserman, *Tetrahedron* **1981**, *37*, 1825–1852.
[29] P. M. Hutchins, R. C. Murphy, *J. Am. Soc. Mass Spectrom.* **2011**, *22*, 867–874.
[30] (a) A. P. Castano, T. N. Demidova, M. R. Hamblin, *Photodiagnosis Photodyn. Ther.* **2004**, *1*, 279-293; (b) J. Moan, K. Berg, *Photochem. Photobio.* **1991**, *53*, 549-533.
[31] (a) E. Cló, J. W. Snyder, P. R. Ogilby, K. V. Gothelf, *ChemBioChem* **2007**, *8*, 475-481; (b) J. W. Snyder, E. Skovsen, J. D. Lambert, L. Poulsen, P. R. Ogilby, *Phys. Chem. Chem. Phys.* **2006,** *8*, 4280-4293; (c) E. Skovsen, J. W. Snyder, J. D. Lambert, P. R. Ogilby, *J. Phys. Chem. B* **2005,** *109*,

8570-8573; (d) P. R. Ogilby, *Chem. Soc. Rev.* **2010**, *39*, 3181-3209; (e) J. W. Snyder, E. Skovsen, J. D. Lambert, P. R. Ogilby, *J. Am. Chem. Soc.* **2005**, *127*, 14558-14559.

[32] (a) J. Garrec, A. Monari, X. Assfeld, L. M. Mir, M. Tarek, *J. Phys. Chem. Lett.* **2014**, *5*, 1653−1658; (b) A. W. Girotti, *J. Lipid Res.* **1998**, *39*, 1529–1542; (c) J. Wong-ekkabut, Z. Xu, W. Triampo, I. M. Tang, D. P. Tieleman, L. Monticelli, *Biophys. J.* **2007**, *93*, 4225–4236; (d) E. Agmon, J. Solon, P. Bassereau, B. R. Stockwell, *Sci. Rep.* **2018**, *8*, 5155; (e) V. Jarerattanachat, M. Karttunen, J. Wong-ekkabut, *J. Phys. Chem. B* **2013**, *117*, 8490−8501.

10.1002/anie.201902815

Entry for the Table of Contents (Please choose one layout)

Layout 1:

COMMUNICATION

Field-induced droplet ionization and acoustic levitation are combined to study the reaction mechanisms of photodynamic therapy for cancer at the air-water interface.

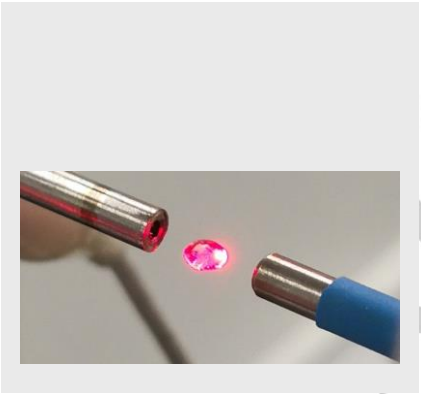

C. Mu, J. Wang, K. M. Barraza, X. Zhang, and J. L. Beauchamp**

Page No. – Page No.

Mass Spectrometric Study of Acoustically Levitated Droplet Illuminates Molecular-Level Mechanism of Photodynamic Therapy for Cancer involving Lipid Oxidation